Computational Mechanics 27 (2001) 75–87 © Springer-Verlag 2001

Analytical study and numerical experiments for true and spurious eigensolutions of a circular cavity using an efficient mixed-part dual BEM

J. T. Chen, I. L. Chung, I. L. Chen

Abstract In this paper, we develop an efficient mixed-part dual BEM to solve the eigensolutions of a circular cavity analytically and numerically. The method is proposed by choosing a fewer number of equations from the dual BEM instead of all of the equations in the dual BEM developed by Chen and his coworkers. To solve this problem analytically, the spurious solution can be filtered out by adding constraints from the dual boundary integral equations. The proposed method is superior to the complex-valued BEM not only for half effort in constructing the influence matrix, but also for its fewer size of dimension. Also, numerical experiments are performed to compare with the analytical results and the true eigensolutions can be easily extracted out in conjunction with the singular value decomposition technique (SVD). The optimum number of collocation point and appropriate collocating positions for the additional constraints are discussed.

1 Introduction

For the Helmholtz eigenproblems, it is well known that the complex-valued boundary element method (BEM) can determine the eigensolutions (Chen et al., 1999a). In determining eigenvalues and eigenmodes for problems with a degenerate boundary (Chen and Chen, 1998), the dual BEM must be resort to overcome the nonunique solution. Nevertheless, complex-valued computation is complex arithematics. To avoid the complex-valued computation, four alternatives, multiple reciprocity method (MRM), real-part BEM, imaginary-part BEM and dual reciprocity method (DRM) have been employed to solve the problems. Tai and Shaw (1974) have tried to solve the Helmholtz eigenproblems using real-part formulation for three-dimensional case. For cavity and plate vibration problems, Hutchinson also employed real-part kernel only (Hutchinson, 1985, 1988, 1991). A simplified method using only real-part kernel was also reported by De Mey (1977). Since only the first eigenvalue was studied in that paper, the spurious solutions were not discovered. Hutchinson found that real-part formulation results in spurious solutions which were filtered out by examining the mode shapes. MRM is also one alternative to solve the problem in real-variable domain. In solving the eigenproblems by using the multiple reciprocity method (MRM), Chen and Wong (1997) also found spurious solutions in a one-dimensional case. Therefore, they pointed out that the MRM formulation is very similar to the real-part BEM formulation. The kernels between the MRM and real-part BEM are almost the same but they can be different from a complementary solution (Chen and Wong, 1997; Yeih et al., 1997). The kernel of MRM is a series form instead of a closed form in the real-part BEM. Kamiya et al. (1996) also pointed out that MRM is no more than real-part formulation. One approach called DRM (Katsikadelis and Nerantzaki, 2000) use only static kernel which is free from the complex-variable computation. According to the experience in the real-part methods, it is expected that spurious solution may also occur since MRM and DRM use the real fundamental solution once the interpolation points are not selected carefully. To extract the true eigensolution, the dual MRM or the real-part dual BEM was proposed to check the residue by substituting the possible eigensolutions into UT (singular) or LM (hypersingular) integral equation (Chen and Wong, 1997; Liou et al., 1999). However, determining boundary modes is a necessary step to find the residue in advance before we distinguish whether the eigenvalue is true or spurious. If the dual formulation is utilized in conjunction with the SVD technique, Yeih et al. (1999a) found the true eigenvalues more efficiently. The eigenproblems of a rod (Yeih et al., 1999a) and a beam (Yeih et al., 1999b) cases were successfully solved. Also, two-dimensional cases were studied (Chen et al., 1999b; Chen et al., 2000a; Kuo et al., 2000). After spurious solutions are filtered out, the true eigensolution can be compared with an analytical solution if available. This is the reason why circular and square cavities were considered in the NTOU BEM Group's papers (Chen and Chen, 1998; Chen et al., 1999a, b; Chen et al., 2000a; Kuo et al., 2000). However, the analytical derivation for spurious solution is not trivial for us to understand why the spurious eigensolution occur. Fortunately, analytical spurious solutions for one-dimensional cases of a rod and a beam have been determined easily (Chen and Wong, 1997; Yeih et al., 1999a, b). To determine the spurious solution for two-dimensional cases analytically, the theory of circulant and degenerate kernel was employed for a circular cavity (Kuo et al., 2000) of a

J. T. Chen (✉), I. L. Chung, I. L. Chen
Department of Harbor and River Engineering,
National Taiwan Ocean University,
Keelung, Taiwan

Financial support from the National Science Council under grant No. NSC-89-2211-E-019-003 for National Taiwan Ocean University is gratefully acknowledged.

discrete system. Many approaches, domain partition technique (Chang, Yeih and Chen, 1999), generalized singular value decomposition (GSVD) (Wu, 1999), CHEEF method (Chen et al., 2000b) have been successfully applied to deal with the spurious solution. Although the real-part BEM is simpler than the complex-valued formulation, the singular and hypersingular integrals should be determined. In order to avoid the singular and hypersingular integrals, imaginary-part BEM (Chen et al., 1999c) was developed. It is interesting to find that the imaginary-part BEM also results in spurious solutions (Chen et al., 1999). Nevertheless, we pay the price of facing the ill-conditioned behavior. Recently, Kang et al. (1999) employed the nondimensional dynamic influence function (NDIF) method to solve the eigenproblem. Chen et al. (2000b) commented that NDIF method is a special case of imaginary-part BEM. To deal with the ill-coditioned problem, Wu (1999) employed the generalized singular value decomposition (GSVD) in conjunction with the Tikhonov technique to regularize the ill-posed problem. Although many approaches in Table 1 have been employed to solve the true and spurious solutions, we may wonder which one is more efficient? From the computational point of view for storage space, we summarize the required dimensions of the available methods in Table 2.

In this paper, we will employ an efficient method to solve for the eigensolution by using the similar concept of CHIEF (combined Helmholtz interior integral equation formulation) (Schenck, 1968) or CHEEF. The main difference between the present formulation and CHIEF or CHEEF method is that we obtain additional constraints from the dual boundary integral equations instead of from the equations on the complementary domain in CHIEF or CHEEF method. The appropriate collocation position and the optimum number of collocation points will be studied analytically and verified numerically. After assembling the sufficient equations, the loss information due to rank deficiency can be recovered. For simplicity, only the Dirichlet case is considered in this paper. The results will be compared with those of analytical solutions, and other numerical methods.

2 Review of the dual BEM for a two-dimensional interior cavity problem

Consider a cavity problem which has the following governing equation:

$$\nabla^2 u(\mathbf{x}) + k^2 u(\mathbf{x}) = 0, \quad \mathbf{x} \in D \ , \tag{1}$$

where D is the domain of cavity, $\mathbf{x}$ is the domain point, k is the wave number, which is the angular frequency over the speed of sound, and $u(x)$ is the acoustic potential. For simplicity, the Dirichlet boundary condition is considered as follows:

$$u(\mathbf{x}) = 0, \quad \mathbf{x} \in B \ , \tag{2}$$

where B denotes the boundary enclosing D. The solution can be described by the following singular integral equation (Chen and Chen, 1998)

$$2\pi u(\mathbf{x}) = \int_B T_c(\mathbf{s},\mathbf{x}) u(\mathbf{s}) \mathrm{d}B(\mathbf{s}) - \int_B U_c(\mathbf{s},\mathbf{x}) \frac{\partial u(\mathbf{s})}{\partial n_\mathbf{s}} \mathrm{d}B(\mathbf{s}), \quad \mathbf{x} \in D \ , \tag{3}$$

where the complex-valued kernel, $T_c(\mathbf{s},\mathbf{x})$, is defined by

$$T_c(\mathbf{s},\mathbf{x}) \equiv \frac{\partial U_c(\mathbf{s},\mathbf{x})}{\partial n_\mathbf{s}} \ , \tag{4}$$

in which $n_\mathbf{s}$ represents the outnormal direction at point $\mathbf{s}$ on the boundary and $U_c(\mathbf{s},\mathbf{x})$ is the fundamental solution. The second one of the dual boundary integral equation for the domain point $\mathbf{x}$ can be derived as follows:

$$2\pi \frac{\partial u(\mathbf{x})}{\partial n_\mathbf{x}} = \int_B M_c(\mathbf{s},\mathbf{x}) u(\mathbf{s}) \mathrm{d}B(\mathbf{s}) - \int_B L_c(\mathbf{s},\mathbf{x}) \frac{\partial u(\mathbf{s})}{\partial n_\mathbf{s}} \mathrm{d}B(\mathbf{s}), \quad \mathbf{x} \in D \ , \tag{5}$$

where

$$L_c(\mathbf{s},\mathbf{x}) \equiv \frac{\partial U_c(\mathbf{s},\mathbf{x})}{\partial n_\mathbf{x}} \ , \tag{6}$$

$$M_c(\mathbf{s},\mathbf{x}) \equiv \frac{\partial^2 U_c(\mathbf{s},\mathbf{x})}{\partial n_\mathbf{x} \partial n_\mathbf{s}} \ , \tag{7}$$

in which $n_\mathbf{x}$ represents the outnormal direction at point $\mathbf{x}$.

By moving the field point $\mathbf{x}$ in Eq. (3) to the smooth boundary, the boundary integral equation for the boundary point can be obtained as follows:

$$\pi u(\mathbf{x}) = \text{C.P.V.} \int_B T_c(\mathbf{s},\mathbf{x}) u(\mathbf{s}) \mathrm{d}B(\mathbf{s}) - \text{R.P.V.} \int_B U_c(\mathbf{s},\mathbf{x}) \frac{\partial u(\mathbf{s})}{\partial n_\mathbf{s}} \mathrm{d}B(\mathbf{s}), \quad \mathbf{x} \in B \ , \tag{8}$$

where C.P.V. is the Cauchy principal value and R.P.V. is the Riemann principal value.

By moving the field point $\mathbf{x}$ in Eq. (5) to a smooth boundary, the boundary integral equations for the boundary point can be obtained as follows:

$$\pi \frac{\partial u(\mathbf{x})}{\partial n_\mathbf{x}} = \text{H.P.V.} \int_B M_c(\mathbf{s},\mathbf{x}) u(s) \mathrm{d}B(\mathbf{s}) - \text{C.P.V.} \int_B L_c(\mathbf{s},\mathbf{x}) \frac{\partial u(\mathbf{s})}{\partial n_\mathbf{s}} \mathrm{d}B(\mathbf{s}), \quad \mathbf{x} \in B \ , \tag{9}$$

where H.P.V. is the Hadamard (Mangler) principal value.

By discretizing the boundary B into boundary elements in Eqs. (8) and (9), we have the algebraic system as follows:

$$\pi\{u\} = [T_c]\{u\} - [U_c]\{t\} \ , \tag{10}$$

$$\pi\{t\} = [M_c]\{u\} - [L_c]\{t\} \ , \tag{11}$$

Table 1. Methods to solve the Helmholtz eigenproblem

	Complex-valued dual BEM	Real-part dual BEM	Imaginary-part dual BEM	Mixed-part dual BEM	Dual MRM
1D rod (residue)					Chen and Wong, 1997
1D rod (SVD)		Yeih et al., 1999a			
1D rod (domain partition)		Chang et al., 1999			
1D beam (SVD)					Yeih et al., 1999b
2D cavity (degenerate boundary and/or double roots)	Chen, and Chen, 1998 (degenerate boundary) Chen et al., 1999a (double roots)				
2D cavity–residue (degenerate boundary)		Liou et al., 1999			Chen and Wong, 1998
2D cavity–SVD (degenerate boundary and/or double roots)		Chen et al., 1999b			Chen et al., 2000a
2D cavity–SVD (analytical derivation for spurious solutions)		Kuo et al., 2000a		Present paper	Kuo, Chung, Chen and Huang 2000b
2D cavity (analytical derivation for ill-posed problem)			Chen, Kuo, Chen and Cheng, 1999 Kuo, Yeih and Wu, 2000		
		Overview, Chen and Hong, 1999			

Each paper has its individual focus as follows:
Chang et al. (1999) The spurious eigensolutions in the real-part BEM are filtered out using the domain partition technique for rod examples
Chen and Chen (1998) The eigenproblem for the two-dimensional Helmholtz problem with or without degenerate boundaries is solved using the complex-valued dual formulation
Chen and Hong (1999) The App. Mech. Rev. article reviews the development of the dual formulation from 1984 to 1999
Chen and Wong (1998) The spurious eigensolutions for a two-dimensional cavity with or without degenerate boundaries are filtered out numerically using the dual MRM in conjunction with the residue method
Chen and Wong (1997) The spurious eigensolutions in the dual MRM are found and filtered out analytically and numerically using the residue method for rod examples. (second order O.D.E.)
Chen et al. (1999a) The degenerate modes for a square cavity are determined numerically using the complex-valued dual BEM
Chen et al. (1999b) This paper focuses on the SVD technique, which can filter out the 2D spurious eigensolutions resulting from the real-part BEM. Also, the multiplicities for double roots are examined
Chen et al. (1999) This paper demonstrates the spurious eigensolutions and ill-posed behavior of imaginary-part BEM by using circulants. Also, the results are compared with the nondimensional dynamic influence function method by Kang, et al
Chen et al. (2000a) This paper focuses on the SVD technique, which can filter out the 2D spurious eigensolutions resulting from the MRM. Also, the multiplicities for double roots are examined
Kuo et al. (2000a) The paper focuses on the analytical derivation for the spurious solutions using the real-part dual BEM
Kuo et al. (2000b) The paper focuses on the analytical derivation for the spurious solutions using the dual MRM. Also, this paper presents a more efficient method with fewer dimension $(N + 2) \times N$ instead of $2N \times N$ in the dual MRM
Kuo et al. (2000c) This paper employed the GSVD technique to determine the true and spurious solutions. Also, the Tikhonov method was utilized to regularized the ill-posed problem
Liou et al. (1999) The spurious eigensolutions for the two-dimensional Helmholtz problem are studied using the real-part dual BEM in conjunction with the residue method
Yeih et al. (1999a) The spurious eigensolutions in the MRM are found and filtered out analytically and numerically using the SVD technique for rod examples. (second order O.D.E.)
Yeih et al. (1999b) The spurious eigensolutions in the MRM are found and filtered out analytically and numerically using the SVD technique for beam examples. (fourth order O.D.E.)
The present paper focuses on the mixed-part dual BEM for determining the eigensolutions

where $[U_c], [T_c], [L_c]$ and $[M_c]$ matrices are the corresponding influence coefficient matrices resulting from the U_c, T_c, L_c and M_c kernels, respectively. The detailed derivation can be found in Chen and Chen (1998). Equations (10) and (11) can be rewritten as

$$[\bar{T}_c]\{u\} = [U_c]\{t\} \ , \tag{12}$$

$$[\bar{L}_c]\{t\} = [M_c]\{u\} \ , \tag{13}$$

where $[\bar{T}_c] = [T_c] - \pi[I]$ and $[\bar{L}_c] = [L_c] + \pi[I]$. For the Dirichlet problem, we can obtain the following equation,

$$[U_c(k)]_{2N\times 2N}\{t\}_{2N\times 1} = \{0\} \ . \tag{14}$$

$$[\bar{L}_c(k)]_{2N\times 2N}\{t\}_{2N\times 1} = \{0\} \ , \tag{15}$$

where $2N$ is the number of boundary elements. For the Neumann problem, the eigenequations obtained from the UT and LM equations in Eqs. (12) and (13) are:

Table 2. Dimension in the methods for solving interior eigenproblems using BEM

	Dimension	Eigensystem			Boundary integral equation
		Eigenvalue	Eigen equation		
			Dirichlet	Neumann	
Complex-valued BEM	$4N \times 2N$	True	$[U_r + iU_i]\{t\} = 0$	$[T_r + iT_i]\{u\} = 0$	$[U_c]\{t\} = [T_c]\{u\}$
Real-part BEM	$2N \times 2N$	True and spurious	$[U_r]\{t\} = 0$	$[\bar{T}_r]\{u\} = 0$	$[U_r]\{t\} = [\bar{T}_r]\{u\}$
Imaginary-part BEM	$2N \times 2N$	True and spurious	$[U_i]\{t\} = 0$	$[T_i]\{u\} = 0$	$[U_i]\{t\} = [T_i]\{u\}$
Dual MRM	$4N \times 2N$	True	$\begin{bmatrix} U_r \\ \bar{L}_r \end{bmatrix}\{t\} = 0$	$\begin{bmatrix} \bar{T}_r \\ M_r \end{bmatrix}\{u\} = 0$	$[U_r]\{t\} = [\bar{T}_r]\{u\}$ $[\bar{L}_r]\{t\} = [M_r]\{u\}$
Real-part dual-BEM	$4N \times 2N$	True	$\begin{bmatrix} U_r \\ \bar{L}_r \end{bmatrix}\{t\} = 0$	$\begin{bmatrix} \bar{T}_r \\ M_r \end{bmatrix}\{u\} = 0$	$[U_r]\{t\} = [\bar{T}_r]\{u\}$ $[\bar{L}_r]\{t\} = [M_r]\{u\}$
CHEEF BEM	$(2N + 2) \times 2N$	True	$\begin{bmatrix} U_r \\ U_{r2} \end{bmatrix}\{t\} = 0$	$\begin{bmatrix} \bar{T}_r \\ \bar{T}_{r2} \end{bmatrix}\{u\} = 0$	$[U_r]\{t\} = [\bar{T}_r]\{u\}$ $[U_{r2}]\{t\} = [\bar{T}_{r2}]\{u\}$
Mixed-part dual-BEM	$(2N + a) \times 2N$	True	$\begin{bmatrix} U_r \\ \bar{L}_{ra} \end{bmatrix}\{t\} = 0$	$\begin{bmatrix} \bar{T}_r \\ M_{ra} \end{bmatrix}\{u\} = 0$	$[U_r]\{t\} = [\bar{T}_r]\{u\}$ $[\bar{L}_r]\{t\} = [M_r]\{u\}$ $[U_i]\{t\} = [\bar{T}_i]\{u\}$ $[\bar{L}_i]\{t\} = [M_i]\{u\}$

U_{r2} and $\bar{T}_{r2}$ are two matrices obtained by collocating two points of the real-part UT equations outside the domain
$\bar{L}_{ra}$ and M_{ra} are two matrices obtained by collocating two boundary points of the real-part LM equations

$$[\bar{T}_c(k)]_{2N\times 2N}\{u\}_{2N\times 1} = \{0\} \ , \tag{16}$$

$$[M_c(k)]_{2N\times 2N}\{u\}_{2N\times 1} = \{0\} \ . \tag{17}$$

To avoid the complex-valued computation, an efficient method will be elaborated on later.

3
An efficient method for an interior two-dimensional acoustic problem in conjunction with SVD technique

For exterior acoustic problems, it is well known that singular and hypersingular complex-valued formulation result in fictitious wave number (Chen, 1998; Chen and Hong, 1999). CHIEF technique is a very popular method to deal with the problem of numerical instability since it can provide sufficient constraints. If interior eigenproblem is solved by using either only real-part or imaginary-part of the complex-valued formulation, spurious solution occurs. A similar method, CHEEF, instead of CHIEF has been applied to deal with the spurious eigensolution. Both CHIEF and CHEEF methods have the same goal to obtain independent constraints by collocating the points in the complementary domain for the integral equation. Based on the CHIEF concept for fictitious frequency, Chen et al. (2000c) extended to solve the spurious eigensolution by using the CHEEF concept. In the CHIEF method, the constraints are obtained using the singular (UT) equation by collocating the point in the complementary domain. However, the present method employs the UT real-part formulation and combines the constraints by collocating the boundary points on either imaginary-part UT, real-part LM or imaginary-part equations. The complex-valued matrice $[U_c]$ can be decomposed into

$$[U_c] = [U_r] + i[U_i] \tag{18}$$

where $i^2 = -1$, $[U_r]$ and $[U_i]$ are the real and imaginary parts, respectively. Similarly, $[\bar{L}_c]$ can be written as

$$[\bar{L}_c] = [\bar{L}_r] + i[\bar{L}_i] \tag{19}$$

where $[\bar{L}_r]$ and $[\bar{L}_i]$ are the real and imaginary parts, respectively. In the MRM or real-part BEM, only $[U_r]$ information is employed to solve for the problem as follows

$$[U_r(k)]_{2N\times 2N}\{t\}_{2N\times 1} = \{0\} \ , \tag{20}$$

However, the rank deficiency of matrice $[U_r(k)]$ occurs since the imaginary-part information is lost. To recover the sufficient information, many approaches can be considered by adding either one of the three equations,

$$[U_i(k)]_{a\times 2N}\{t\}_{2N\times 1} = \{0\} \ , \tag{21}$$

$$[\bar{L}_r(k)]_{a\times 2N}\{t\}_{2N\times 1} = \{0\} \ , \tag{22}$$

$$[\bar{L}_i(k)]_{a\times 2N}\{t\}_{2N\times 1} = \{0\} \ , \tag{23}$$

where a is the number of selected equations, $[U_i(k)]$, $[\bar{L}_r(k)]$ and $[\bar{L}_i(k)]$ matrices are obtained from the dual formulation. To filter out spurious eigenvalues using the SVD technique, we can combine Eq. (20) with either one of Eqs. (21)–(23) together to obtain an overdeterminate system

$$[G(k)]_{(2N+a)\times 2N}\{t\}_{2N\times 1} = \{0\} \ , \tag{24}$$

where the $[G(k)]$ is a assembled matrix with a dimension $(2N + a)$ by $2N$, which can be assembled by the $[U_r(k)]$ and any one additional matrix, of $[U_i(k)]$, $[\bar{L}_r(k)]$ and $[\bar{L}_i(k)]$ matrices as shown below:

$$[G(k)]_{(2N+a)\times 2N} = \begin{bmatrix} U_r(k) \\ U_i(k) \end{bmatrix}_{(2N+a)\times 2N}$$

for the Dirichlet problem. (25)

$$[G(k)]_{(2N+a)\times 2N} = \begin{bmatrix} U_{\mathrm{r}}(k) \\ \bar{L}_{\mathrm{r}}(k) \end{bmatrix}_{(2N+a)\times 2N}$$
for the Dirichlet problem. (26)

$$[G(k)]_{(2N+a)\times 2N} = \begin{bmatrix} U_{\mathrm{r}}(k) \\ \bar{L}_{\mathrm{i}}(k) \end{bmatrix}_{(2N+a)\times 2N}$$
for the Dirichlet problem. (27)

As for the true eigenvalues, the rank of the $[G(k)]$ matrix with a dimension $(2N + a)$ by $2N$ must at most be $2N - 1$ to have a nontrivial solution. As for the spurious eigenvalues, the rank must be $2N$ to obtain a trivial solution. Based on this criterion, the SVD technique can be employed to detect the true eigenvalues by checking whether or not the first minimum singular value, σ_1, is zero. Since discretization creates errors, very small values for σ_1, but not exactly zeros, will be obtained when k is near the critical wave number. In order to avoid determining the threshold for the zero numerically, a value of σ_1 closer to zero must be obtained using a smaller increment near the critical wave number, k. Such a value is confirmed to be a true eigenvalue. For the true eigenvalues with a multiplicity of two, we can consider the eigenvalues which make $\sigma_2 = 0$ and $\sigma_1 = 0$ at the same k value.

Since the matrices in Eqs. (25)–(27) are overdetermined, we will consider a linear algebra problem with more number of equations than unknowns:

$$[\mathbf{A}]_{m\times n}\{\mathbf{x}\}_{n\times 1} = \{\mathbf{b}\}_{m\times 1}, \quad m > n \ , \tag{28}$$

where m is the number of equations, n is the number of unknowns and $[\mathbf{A}]$ is the leading matrix, which can be decomposed into

$$[\mathbf{A}]_{m\times n} = [\mathbf{\Phi}]_{m\times m}[\mathbf{\Sigma}]_{m\times n}[\mathbf{\Psi}]^{\mathrm{T}}_{n\times n} \ , \tag{29}$$

where $[\mathbf{\Phi}]$ is a left unitary matrix constructed by the left singular vectors $(\phi_1, \phi_2, \phi_3, \ldots, \phi_m)$, $[\mathbf{\Sigma}]$ is a diagonal matrix which has singular values $\sigma_1, \sigma_2, \ldots,$ and σ_n allocated in a diagonal line as

$$[\mathbf{\Sigma}] = \begin{bmatrix} \sigma_n & \cdots & 0 \\ \vdots & \ddots & \vdots \\ 0 & \cdots & \sigma_1 \\ 0 & \cdots & 0 \\ 0 & \cdots & 0 \end{bmatrix}, \quad m > n \ , \tag{30}$$

in which $\sigma_n \geq \sigma_{n-1} \geq \cdots \geq \sigma_1$ and $[\mathbf{\Psi}]^{\mathrm{T}}$ is the complex conjugate transpose of a right unitary matrix constructed by the right singular vectors $(\psi_1, \psi_2, \psi_3, \ldots, \psi_n)$. As we can see in Eq. (30), there exists at most n nonzero singular values. This means that we can find at most n linear independent equations in the system of equations. If we have p zero singular values $(0 \leq p \leq n)$, this means that the rank of the system of equations is equal to $n - p$. However, the singular value may be very close to zero numerically, resulting in rank deficiency. For a general eigenproblem as shown in this paper, the $[G(k)]$ matrix with dimension $(2N + a)$ by $2N$ will have a rank of $2N - 1$ for the true eigenvalue with multiplicity 1 and $\sigma_1 = 0$ theoretically. For the true eigenvalues with multiplicity Q, the rank of $[G(k)]$ will be reduced to $2N - Q$ in which $\sigma_1, \sigma_2, \ldots,$ and σ_Q are zeros theoretically. In another words, the matrix has a nullity of Q. In the case of spurious eigenvalues, the rank for the $[G(k)]$ matrix is $2N$, and the minimum singular value is not zero. Determining the eigenvalues of the system of equations has now been transformed into finding the values of k which make the rank of the leading coefficient matrix smaller than $2N$. This means that when $m = 2N + a, n = 2N$ and $\mathbf{b}_{(2N+a)\times 1} = 0$. The true case will make $p \geq 1$, such that the minimum singular values must be zero or very close to zero.

Since we have employed the SVD technique to filter out the spurious eigenvalues, we can obtain the boundary mode by extracting the right unitary vector in SVD. According to the definition of SVD, we have

$$[A]\psi_p = \sigma_p\phi_p, \quad p = 1, 2, 3, \ldots, n \ . \tag{31}$$

where ϕ and ψ are the left and right unitary vectors. By choosing the qth zero singular value, σ_q and substituting the qth right eigenvector, ψ_q, into Eq. (31), we have

$$[A]\psi_q = 0\phi_q = 0, \quad q = 1, 2, 3, \ldots, Q \ . \tag{32}$$

According to Eq. (32), the nontrivial boundary mode is found to be the column vector of ψ_q in the right unitary matrix.

When we take all the $2N + a$ sufficient equations into account, which apparently causes the rank of the leading coefficient matrix to be equal to $2N - 1$ for the true eigenvalue with multiplicity 1. The boundary modes can be obtained from the $[\mathbf{\Psi}]$ matrix in Eq. (29) using the SVD technique. Another advantage for using the SVD is that it can determine the multiplicities for the true eigenvalues by finding the number of successive zeros in the singular values.

4 Analytical study of a circular cavity for choosing the optimal points using mixed-part dual BEM

The explicit forms for the complex-valued U_{c} and L_{c} kernels can be expressed as

$$U_{\mathrm{c}}(\mathbf{s}, \mathbf{x}) = \frac{-i\pi H_0^{(1)}(kr)}{2} \tag{33}$$

$$L_{\mathrm{c}}(\mathbf{s}, \mathbf{x}) = \frac{-i\pi \partial H_0^{(1)}(kr)}{2\partial\rho} \tag{34}$$

where $H_0^{(1)}$ is the first kind Hankel function of zeroth order. Based on the polar coordinate, the field point and source point can be rewritten as $\mathbf{x} = (\rho, \phi)$ and $\mathbf{s} = (R, \theta)$ as shown in Fig. 1. Since $\mathbf{x}$ and $\mathbf{s}$ are on the boundaries of radius ρ and R. respectively, $U_{\mathrm{r}}(\mathbf{s}, \mathbf{x})$ can be expanded into degenerate form as follows:

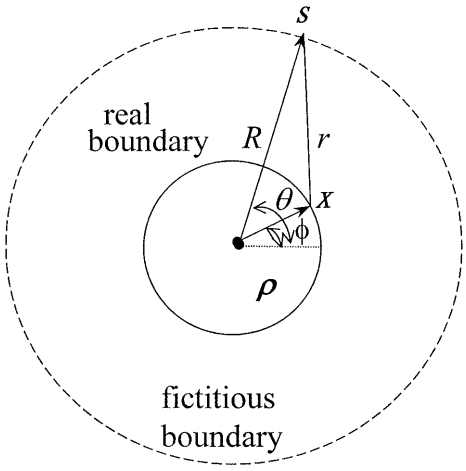

Fig. 1. The definitions of ρ, θ, ϕ, r and R

$$U_{\mathrm{r}}(\mathbf{s},\mathbf{x}) = \mathrm{Real}[U_{\mathrm{c}}(\mathbf{s},\mathbf{x})] = \begin{cases} U(R,\theta;\rho,0) \\ \quad = \sum_{-\infty}^{\infty} \frac{\pi}{2} Y_n(kR) J_n(k\rho)\cos(n\theta), & R > \rho, \\ U(R,\theta;\rho,0) \\ \quad = \sum_{-\infty}^{\infty} \frac{\pi}{2} Y_n(k\rho) J_n(kR)\cos(n\theta), & R < \rho, \end{cases} \tag{35}$$

Similarly, we have

$$U_{\mathrm{i}}(\mathbf{s},\mathbf{x}) = \mathrm{Imag}[U_{\mathrm{c}}(\mathbf{s},\mathbf{x})] = \begin{cases} U(R,\theta;\rho,0) \\ \quad = \sum_{-\infty}^{\infty} \frac{-\pi}{2} J_n(kR) J_n(k\rho)\cos(n\theta), & R > \rho, \\ U(R,\theta;\rho,0) \\ \quad = \sum_{-\infty}^{\infty} \frac{-\pi}{2} J_n(k\rho) J_n(kR)\cos(n\theta), & R < \rho, \end{cases} \tag{36}$$

$$L_{\mathrm{r}}(\mathbf{s},\mathbf{x}) = \mathrm{Real}[L_{\mathrm{c}}(\mathbf{s},\mathbf{x})] = \begin{cases} L_{\mathrm{r}}(R,\theta;\rho,0) \\ \quad = \sum_{-\infty}^{\infty} \frac{\pi}{2} Y_n\prime(kR) J_n(k\rho)\cos(n\theta), & R > \rho, \\ L_{\mathrm{r}}(R,\theta;\rho,0) \\ \quad = \sum_{-\infty}^{\infty} \frac{\pi}{2} Y_n\prime(k\rho) J_n(kR)\cos(n\theta), & R < \rho, \end{cases} \tag{37}$$

$$L_{\mathrm{i}}(\mathbf{s},\mathbf{x}) = \mathrm{Imag}[L_{\mathrm{c}}(\mathbf{s},\mathbf{x})] = \begin{cases} L_{\mathrm{i}}(R,\theta;\rho,0) \\ \quad = \sum_{-\infty}^{\infty} \frac{\pi}{2} J_n\prime(kR) J_n(k\rho)\cos(n\theta), & R > \rho, \\ L_{\mathrm{i}}(R,\theta;\rho,0) \\ \quad = \sum_{-\infty}^{\infty} \frac{\pi}{2} J_n\prime(k\rho) J_n(kR)\cos(n\theta), & R < \rho, \end{cases} \tag{38}$$

where Real and Imag denote the real and imaginary parts, respectively. Equations (35)–(38) show that source point $\mathbf{s}$ and field point $\mathbf{x}$ in the two-point function are separated and $J_n(k\rho)$ is the *nth* order Bessel function of the first kind and $Y_n(k\rho)$ is the nth order Bessel function of the second kind. Equations (35)–(38) can also be derived through the addition theorem for the Hankel function. By superimposing $2N$ constant source distribution $\{\bar{t}\}$ along the fictitious boundary with radius R and collocating the $2N$ points on the boundary with radius ρ, we have

$$[U_{\mathrm{r}}]\{\bar{t}\} = \begin{bmatrix} a_0 & a_1 & a_2 & \cdots & a_{2N-2} & a_{2N-1} \\ a_{2N-1} & a_0 & a_1 & \cdots & a_{2N-3} & a_{2N-2} \\ a_{2N-2} & a_{2N-1} & a_0 & \cdots & a_{2N-4} & a_{2N-3} \\ \vdots & \vdots & \vdots & \ddots & \vdots & \vdots \\ a_1 & a_2 & a_3 & \cdots & a_{2N-1} & a_0 \end{bmatrix} \times \begin{Bmatrix} \bar{t}_0 \\ \bar{t}_1 \\ \bar{t}_2 \\ \vdots \\ \bar{t}_{2N-1} \end{Bmatrix} = \{0\} \tag{39}$$

for the Dirichlet problem, where $\bar{t}_j$ is the boundary density of single layer potential distributed on the boundary with radius R, and $[U_{\mathrm{r}}]$ is the influence matrix with the elements shown below:

$$a_m = \int_{(m-\frac{1}{2})\Delta\theta}^{(m+\frac{1}{2})\Delta\theta} U_{\mathrm{r}}(R,\theta;\rho,0) R\,\mathrm{d}\theta \approx U_{\mathrm{r}}(R,\theta_m;\rho,0) R\Delta\theta, \quad m = 0,1,2,\ldots,2N-1 \tag{40}$$

where $\Delta\theta = 2\pi/2N$ and $\theta_m = m\Delta\theta$.

The matrix $[U_{\mathrm{r}}]$ in Eq. (39) is found to be circulants since rotation symmetry for the influence coefficients are considered. By introducing the following bases for the circulants $I, C_{2N}^1, C_{2N}^2, \ldots, C_{2N}^{2N-1}$, we can expand $[U_{\mathrm{r}}]$ into

$$[U_{\mathrm{r}}] = a_0 I + a_1 C_{2N}^1 + a_2 C_{2N}^2 + \cdots + a_{2N-1} C_{2N}^{2N-1} \tag{41}$$

where I is a unit matrix and

$$C_{2N} = \begin{bmatrix} 0 & 1 & 0 & \cdots & 0 & 0 \\ 0 & 0 & 1 & \cdots & 0 & 0 \\ \vdots & \vdots & \vdots & \ddots & \vdots & \vdots \\ 0 & 0 & 0 & \cdots & 0 & 1 \\ 1 & 0 & 0 & \cdots & 0 & 0 \end{bmatrix}_{2N\times 2N} \tag{42}$$

Based on the theory of circulants (Goldberg, 1991), the spectral properties for the influence matrices, U_{r}, can be easily found as follows:

$$\lambda_\ell = a_0 + a_1\alpha_\ell + a_2\alpha_\ell^2 + \cdots + a_{2N-1}\alpha_\ell^{2N-1}, \quad \ell = 0, \pm1, \pm2, \ldots, \pm(N-1), N \tag{43}$$

where λ_ℓ and α_ℓ are the eigenvalues for $[U_{\mathrm{r}}]$ and $[C_{2N}]$, respectively. It is easily found that the eigenvalues for the circulants $[C_{2N}]$ are the roots for $\alpha^{2N} = 1$ as shown below:

$$\alpha_l = \mathrm{e}^{\mathrm{i}2\pi l/2N}, \quad l = 0, \pm1, \pm2, \ldots, \pm(N-1), N \text{ or } l = 0,1,2,\ldots,2N-1\ , \tag{44}$$

and the eigenvectors are

$$\{\phi_l\} = \begin{Bmatrix} 1 \\ \alpha_l \\ \alpha_l^2 \\ \alpha_l^3 \\ \vdots \\ \alpha_l^{2N-1} \end{Bmatrix} , \tag{45}$$

respectively.

Substituting Eq. (44) into Eq. (43), we have

$$\lambda_\ell = \sum_{m=0}^{2N-1} a_m \alpha_\ell^m = \sum_{m=0}^{2N-1} a_m \mathrm{e}^{\mathrm{i}2\pi m\ell/(2N)}, \quad \ell = 0, \pm1, \pm2, \ldots, \pm(N-1), N_x \ . \tag{46}$$

According to the definition for a_m in Eq. (40), we have

$$a_m = a_{2N-m}, \quad m = 0, 1, 2, \ldots, 2N-1 \ . \tag{47}$$

Substituting Eq. (47) into Eq. (46), we have

$$\lambda_\ell = a_0 + (-1)^\ell a_N + \sum_{m=1}^{N-1} (\alpha_\ell^m + \alpha_\ell^{2N-m}) a_m = \sum_{m=0}^{2N-1} \cos(m\ell\Delta\theta) a_m \ . \tag{48}$$

Substituting Eq. (40) into Eq. (48), we have

$$\lambda_\ell \approx \sum_{m=0}^{2N-1} \cos(m\ell\Delta\theta) U_\mathrm{r}(R, m\Delta\theta; \rho, 0) R\Delta\theta \tag{49}$$

As N approaches infinity, the Riemann sum of Eq. (49) can be transformed to the following integral

$$\lambda_\ell = \int_0^{2\pi} \cos(\ell\theta) \sum_{m=-\infty}^{\infty} \frac{\pi}{2} Y_m(kR) J_m(k\rho) \cos\, m\theta R \, \mathrm{d}\theta = \pi^2 R Y_\ell(kR) J_\ell(k\rho) \tag{50}$$

Since the wave number k is imbedded in each element of the $[U_\mathrm{r}]$ matrix, the eigenvalues for $[U_\mathrm{r}]$ are also functions of k. Finding the eigenvalues for the Helmholtz equation or finding the zeros for the determinant of $[U_\mathrm{r}]$ is equal to finding the zeros for multiplication of all the eigenvalues of $[U_\mathrm{r}]$. Based on the following equation:

$$\det[U_\mathrm{r}] = \lambda_0 \lambda_N (\lambda_1 \lambda_2 \cdots \lambda_{N-1})(\lambda_{-1} \lambda_{-2} \cdots \lambda_{-(N-1)}) \ , \tag{51}$$

the possible eigenvalues (true or spurious) occur at

$$Y_\ell(kR) J_\ell(k\rho) = 0, \quad \ell = 0, \pm1, \pm2, \ldots, \pm(N-1), N \ . \tag{52}$$

The value k satisfying Eq. (52) may be possible eigenvalues, either spurious eigenvalues or true eigenvalues. Here we adopt the similar concept of CHIEF or CHEEF method to filter out the spurious eigenvalues. By collocating the boundary point on $\mathbf{x}_1 = (\rho_1, \phi_1)$ for Eqs. (21)–(23), we have

$$0 = \int_B U_\mathrm{i}(s, x) t(s) \mathrm{d}B(s) = [w_{1,a}^\mathrm{T}]\{t\} \ , \tag{53}$$

$$0 = \int_B L_\mathrm{r}(s, x) t(s) \mathrm{d}B(s) = [w_{1,b}^\mathrm{T}]\{t\} \ , \tag{54}$$

$$0 = \int_B L_\mathrm{i}(s, x) t(s) \mathrm{d}B(s) = [w_{1,c}^\mathrm{T}]\{t\} \ , \tag{55}$$

where $[w_1^\mathrm{T}] = (w_1^1, w_1^2, w_1^3, \ldots, w_1^{2N})$ is the row vector of the influence matrix by collocating the boundary point $\mathbf{x}_1$. Combining Eq. (39) and either one of Eqs. (53)–(55), we obtain an overdetermined system

$$\begin{bmatrix} U_\mathrm{r}(k) \\ w_{1,i}^\mathrm{T}(k) \end{bmatrix} \{t\} = \{0\} \tag{56}$$

where $\{t\} = \{\phi_n\}$ and i can be either, a, b, or c. The additional constraints, $[w_{1,i}^\mathrm{T}]\{t\} = 0$, $i = a, b$ and c provide the discriminant, $\triangle$, to be

$$\triangle_{U_\mathrm{i}}^{(1)} = [w_{1,a}^\mathrm{T}]\{t\} = \pi^2 \rho_1 J_n(k\rho) J_n(k\rho) \mathrm{e}^{\mathrm{i}n\phi_1} \ , \tag{57}$$

$$\triangle_{L_\mathrm{r}}^{(1)} = [w_{1,b}^\mathrm{T}]\{t\} = \pi^2 \rho_1 Y_n'(k\rho) J_n(k\rho) \mathrm{e}^{\mathrm{i}n\phi_1} \ , \tag{58}$$

$$\triangle_{L_\mathrm{i}}^{(1)} = [w_{1,c}^\mathrm{T}]\{t\} = \pi^2 \rho_1 J_n'(k\rho) J_n(k\rho) \mathrm{e}^{\mathrm{i}n\phi_1} \ , \tag{59}$$

where the superscript "(1)" denotes one additional constraint. In case of single spurious case, we have the spurious eigenvalue k_s such that $Y_0(k_\mathrm{s}\rho) = 0$ as shown in Eq. (52). By adding any one of Eqs. (53)–(55), the spurious eigenvalues cannot pass the zero test of Eqs. (57)–(59) since the discriminant is never zero. Thus, we can filter out for a single spurious eigenvalue by choosing anyone of Eqs. (57)–(59).

In another words, the intersection set between Eq. (52) and either one of Eqs. (57)–(59) for the solution is true. For double spurious eigenvalues $k_{n,m}$, we have $Y_n(k_{n,m}) = 0$, $n \geq 1$. If we adopt two boundary points, $\mathbf{x}_1$ and $\mathbf{x}_2$, on a radial distance $\rho = \rho_1 = \rho_2$, and combine with Eq. (39), we have

$$\begin{bmatrix} U_\mathrm{r}(k) \\ w_1^\mathrm{T}(k) \\ w_2^\mathrm{T}(k) \end{bmatrix} \{t\} = \{0\} \ , \tag{60}$$

where $[w_2^\mathrm{T}] = (w_2^1, w_2^2, w_2^3, \ldots, w_2^{2N})$ is the row vector of the influence matrix by collocating the second point for the boundary integral equations. When the spurious eigenvalues have a multiplicity two, we need two additional constraints

$$\begin{bmatrix} w_1^\mathrm{T}(k) \\ w_2^\mathrm{T}(k) \end{bmatrix} \{t\} = \begin{bmatrix} w_1^\mathrm{T} \\ w_2^\mathrm{T} \end{bmatrix} \{\alpha t_1 + \beta t_2\} = \begin{bmatrix} w_1^\mathrm{T} t_1 & w_1^\mathrm{T} t_2 \\ w_2^\mathrm{T} t_1 & w_2^\mathrm{T} t_2 \end{bmatrix} \begin{Bmatrix} \alpha \\ \beta \end{Bmatrix} \ , \tag{61}$$

where $t = \alpha t_1 + \beta t_2$, $\{t_1\} = \{\phi_n\}$ and its conjugate $\{t_2\} = \{\phi_n^*\}$ are two independent boundary modes, α and β are two arbitrary constants. The four elements in the matrice of Eq. (61) are

$$w_1^\mathrm{T} t_1^\mathrm{T} = \pi^2 \rho J_n(k\rho) J_n(k\rho) \mathrm{e}^{\mathrm{i}n\phi_1} \ , \tag{62}$$

$$w_1^\mathrm{T} t_2^\mathrm{T} = \pi^2 \rho J_n(k\rho) J_n(k\rho) \mathrm{e}^{-\mathrm{i}n\phi_1} \ , \tag{63}$$

Table 3. True and spurious systems for the Dirichlet problem using the complex, real-part and imaginary-part BEMs

			Real U part	Real L part	Imag U part	Imag L part
1D bar	Eigenvalue	True	sin[k]	sin[k]	sin[k]	sin[k]
		Spurious	sin[k]	sin[k]	sin[k]	sin[k]
2D circular membrane	Eigenvalue	True	J	J	J	J
		Spurious	Y	Y′	J	J′

$$w_2^{\mathrm{T}} t_1^{\mathrm{T}} = \pi^2 \rho J_n(k\rho) J_n(k\rho) \mathrm{e}^{\mathrm{i}n\phi_2} \ , \tag{64}$$

$$w_2^{\mathrm{T}} t_2^{\mathrm{T}} = \pi^2 \rho J_n(k\rho) J_n(k\rho) \mathrm{e}^{-\mathrm{i}n\phi_2} \ . \tag{65}$$

if additional equations are obtained from U_{i} kernel. Eqs. (62)–(65) changed to

$$w_1^{\mathrm{T}} t_1^{\mathrm{T}} = \pi^2 \rho Y_n'(k\rho) J_n(k\rho) \mathrm{e}^{\mathrm{i}n\phi_1} \ , \tag{66}$$

$$w_1^{\mathrm{T}} t_2^{\mathrm{T}} = \pi^2 \rho Y_n'(k\rho) J_n(k\rho) \mathrm{e}^{-\mathrm{i}n\phi_1} \ , \tag{67}$$

$$w_2^{\mathrm{T}} t_1^{\mathrm{T}} = \pi^2 \rho Y_n'(k\rho) J_n(k\rho) \mathrm{e}^{\mathrm{i}n\phi_2} \ , \tag{68}$$

$$w_2^{\mathrm{T}} t_2^{\mathrm{T}} = \pi^2 \rho Y_n'(k\rho) J_n(k\rho) \mathrm{e}^{-\mathrm{i}n\phi_2} \ . \tag{69}$$

if additional equations are obtained from $\bar{L}_{\mathrm{r}}$ kernel. Similarly, we have

$$w_1^{\mathrm{T}} t_1^{\mathrm{T}} = \pi^2 \rho J_n'(k\rho) J_n(k\rho) \mathrm{e}^{\mathrm{i}n\phi_1} \ , \tag{70}$$

$$w_1^{\mathrm{T}} t_2^{\mathrm{T}} = \pi^2 \rho J_n'(k\rho) J_n(k\rho) \mathrm{e}^{-\mathrm{i}n\phi_1} \ , \tag{71}$$

$$w_2^{\mathrm{T}} t_1^{\mathrm{T}} = \pi^2 \rho J_n'(k\rho) J_n(k\rho) \mathrm{e}^{\mathrm{i}n\phi_2} \ , \tag{72}$$

$$w_2^{\mathrm{T}} t_2^{\mathrm{T}} = \pi^2 \rho J_n'(k\rho) J_n(k\rho) \mathrm{e}^{-\mathrm{i}n\phi_2} \ . \tag{73}$$

if additional equations are obtained from $\bar{L}_{\mathrm{i}}$ kernel. Since the spurious double roots make the rank less than 2, the additional two equations for the imaginary-part $[U_{\mathrm{i}}]$ kernels must provide independent constraints, such that

$$\begin{bmatrix} \pi^2 \rho J_n(k\rho) J_n(k\rho) \mathrm{e}^{\mathrm{i}n\phi_1} & \pi^2 \rho J_n(k\rho) J_n(k\rho) \mathrm{e}^{-\mathrm{i}n\phi_1} \\ \pi^2 \rho J_n(k\rho) J_n(k\rho) \mathrm{e}^{\mathrm{i}n\phi_2} & \pi^2 \rho J_n(k\rho) J_n(k\rho) \mathrm{e}^{-\mathrm{i}n\phi_2} \end{bmatrix} \begin{bmatrix} \alpha \\ \beta \end{bmatrix} \neq 0 \ . \tag{74}$$

If they are dependent, we have the determinant

$$\begin{aligned} \triangle_{U_{\mathrm{i}}}^{(2)} &= \det \begin{vmatrix} \pi^2 \rho J_n(k\rho) J_n(k\rho) \mathrm{e}^{\mathrm{i}n\phi_1} & \pi^2 \rho J_n(k\rho) J_n(k\rho) \mathrm{e}^{-\mathrm{i}n\phi_1} \\ \pi^2 \rho J_n(k\rho) J_n(k\rho) \mathrm{e}^{\mathrm{i}n\phi_2} & \pi^2 \rho J_n(k\rho) J_n(k\rho) \mathrm{e}^{-\mathrm{i}n\phi_2} \end{vmatrix} \\ &= \rho^2 J_n(k\rho) J_n(k\rho) J_n(k\rho) J_n(k\rho) (\mathrm{e}^{\mathrm{i}n(\phi_1 - \phi_2)} - \mathrm{e}^{-\mathrm{i}n(\phi_1 - \phi_2)}) \\ &= \rho^2 J_n(k\rho) J_n(k\rho) J_n(k\rho) J_n(k\rho) 2\mathrm{i} \sin(n\phi) \\ &= 0, \end{aligned} \tag{75}$$

where the superscript "(2)" denotes two additional constraints and $\phi = \phi_1 - \phi_2$ indicates the intersecting angle between the two boundary points. Similarly, we can obtain

$$\triangle_{L_{\mathrm{r}}}^{(2)} = \rho^2 Y_n'(k\rho) Y_n'(k\rho) J_n(k\rho) J_n(k\rho) 2\mathrm{i} \sin(n\phi) = 0 \ , \tag{76}$$

$$\triangle_{L_{\mathrm{i}}}^{(2)} = \rho^2 J_n'(k\rho) J_n'(k\rho) J_n(k\rho) J_n(k\rho) 2\mathrm{i} \sin(n\phi) = 0 \ , \tag{77}$$

The discriminant $\triangle$ indicates,

1. If only one additional constraint is obtained, then we can succeed in filtering out the single spurious roots of zeros for $Y_0(k\rho)$.
2. If the two selected points with intersection angle ϕ makes $n\phi = \pi$, we fail to filter out the double spurious roots for the zeros of $Y_n(k\rho) = 0, n \geq 1$.
3. No more than two points are required if the collocation points are properly chosen.

5 Numerical examples

A circular cavity with a radius $(\rho = 1)$ subject to the Dirichlet boundary condition $(u = 0, \rho = 1)$ is considered. In this case, an analytical solution is available (Chen et al., 1999b, c). The true and spurious eigensolutions are summarized in Table 3. True eigenvalues satisfy $J_m(k) = 0, \quad m = 0, 1, 2, 3, \ldots$. Forty elements are adopted in the boundary element mesh. Since two alternatives, the UT or LM equations, can be used to collocate on the boundary, two results from the real-part UT and real-part LM methods can be obtained. Figure 2 shows the minimum singular value versus k using real-part UT method. The true eigenvalue contaminated by spurious eigenvalues can be obtained as shown in Fig. 2 by considering the near zero minimum singular value if only the real-part UT equation is chosen. The true eigenvalues occur at the positions of zeros for $J_m(k)$ while the spurious eigenvalues occur at the positions of zeros for $Y_m(k)$. J_m^n and Y_m^n in Fig. 2 denote the possible roots for k which satisfy $J_m(k) = 0$ and $Y_m(k) = 0$, respectively. Figure 3 shows the second minimum singular value versus

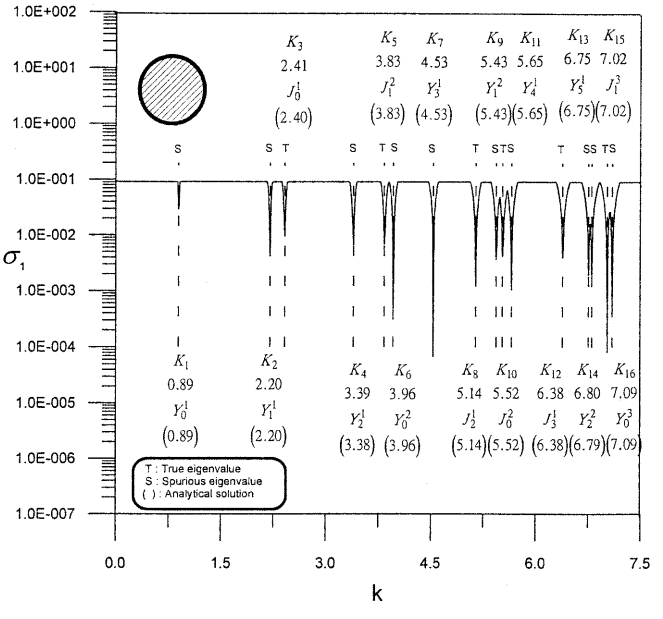

Fig. 2. The first minimum singular values σ_1 versus k using the $[U]$ matrices of real-part dual BEM for the Dirichlet problem

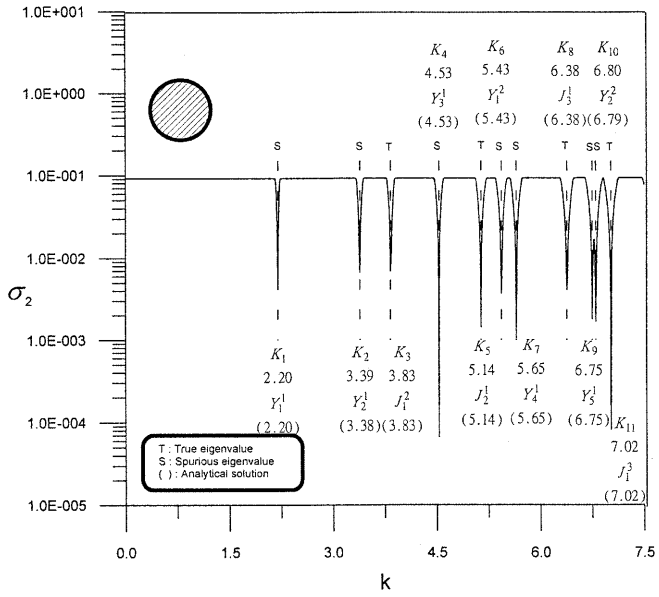

Fig. 3. The second minimum singular values σ_2 versus k using the $[U]$ matrices of real-part dual BEM for the Dirichlet problem

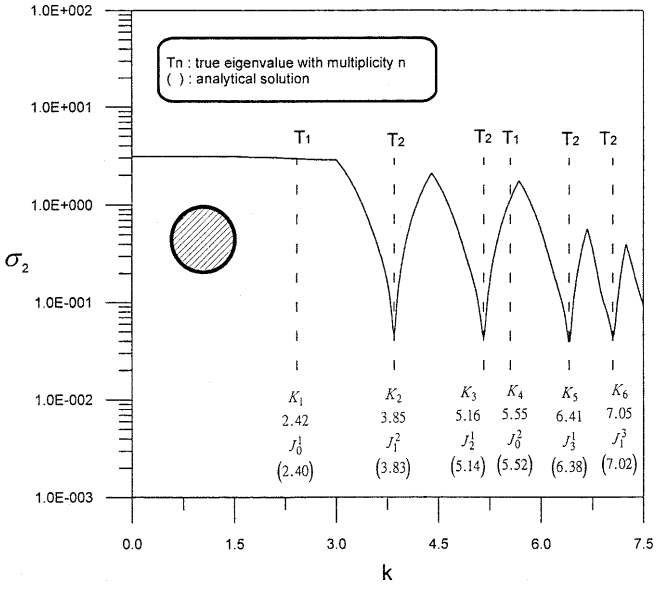

Fig. 5. The second minimum singular values σ_2 versus k using the $\begin{bmatrix} U \\ L \end{bmatrix}$ matrices of real-part dual BEM for the Dirichlet problem

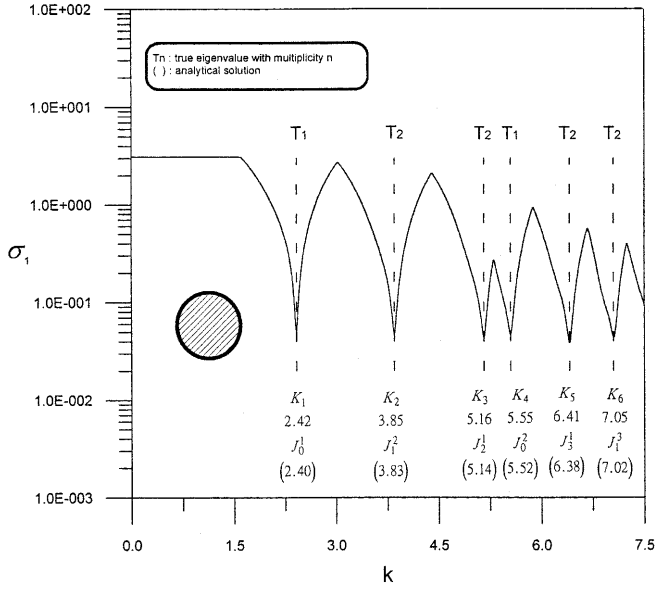

Fig. 4. The first minimum singular values σ_1 versus k using the $\begin{bmatrix} U \\ L \end{bmatrix}$ matrices of real-part dual BEM for the Dirichlet problem

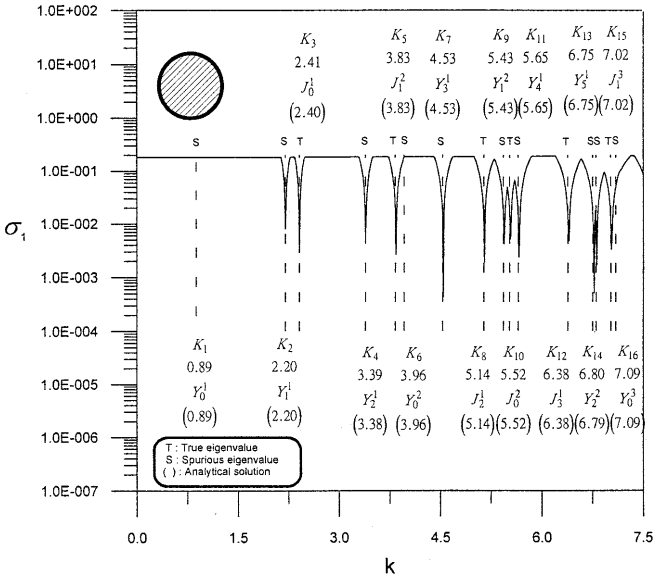

Fig. 6. The first minimum singular values σ_1 versus k using the $\begin{bmatrix} U_r \\ U_i \end{bmatrix}$ matrices of dual BEM for the Dirichlet problem

k when only using real-part UT equation. It is interesting to find that no spurious eigenvalues occur as shown in Fig. 4, when the UT and LM equations are combined together. After obtaining the true eigenvalues, their multiplicities can be determined as shown in Fig. 5 from the locations where the second minimum singular values also approach zero. It is found that double roots are present in this case. All the above results are obtained by considering all the equations in the dual formulation.

Using the present approach, one additional equation from $[U_i]$ in conjunction with $[U_r]_{2N\times 2N}$ matrice can be employed to filter out the single spurious eigenvalue of $Y_0(k) = 0$ as shown in Fig. 6. It is found that the single spurious eigenvalues ($Y_0^1(0.89)$, $Y_0^2(3.96)$ and $Y_0^3(7.09)$) are successfully filtered out. However, the double spurious eigenvalues ($Y_1^1(2.20)$, $Y_2^1(3.38)$, $Y_3^1(4.53)$, $Y_1^2(5.43)$, etc) still appear as predicted. By replacing the constraint from $[U_i]$ to either $[\bar{L}_i]$ or $[\bar{L}_r]$, we have the results shown in Figs. 7 and 8, respectively. Some single spurious eigenvalues at high wave number in Fig. 7 cannot be filtered out in the discrete system for the limited number of boundary elements. Also, the second single spurious eigenvalue ($Y_0^2(3.96)$) was not successfully filtered out in Fig. 8. The reason may be explained by the fewer number of elements. By replacing the basic equations of $[U_r]_{2N\times 2N}$ to $[\bar{L}_r]_{2N\times 2N}$ in

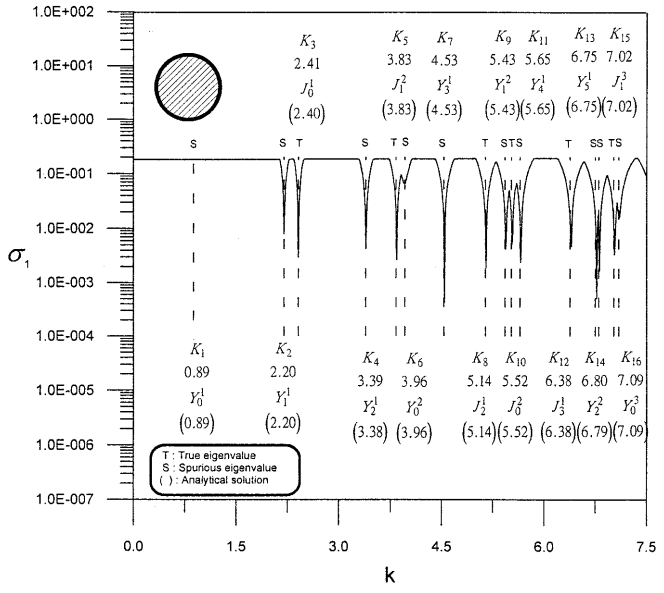

Fig. 7. The first minimum singular values σ_1 versus k using the $\begin{bmatrix} U_r \\ \bar{L}_i \end{bmatrix}$ matrices the of dual BEM for the Dirichlet problem

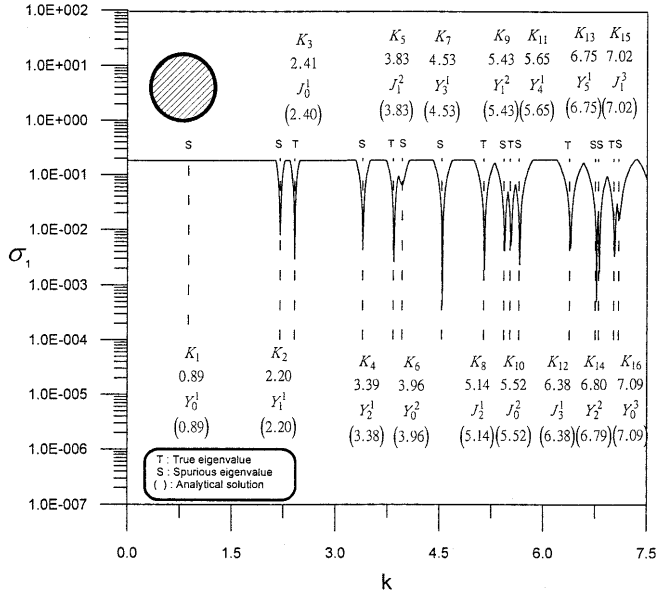

Fig. 8. The first minimum singular values σ_1 versus k using the $\begin{bmatrix} U_r \\ \bar{L}_r \end{bmatrix}$ matrices of dual BEM for the Dirichlet problem

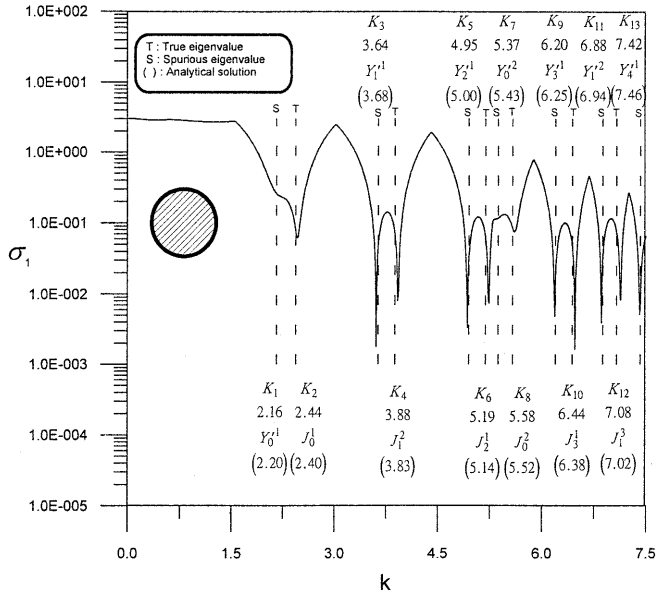

Fig. 9. The first minimum singular values σ_1 versus k using the $\begin{bmatrix} \bar{L}_r \\ \bar{L}_i \end{bmatrix}$ matrices of dual BEM for the Dirichlet problem

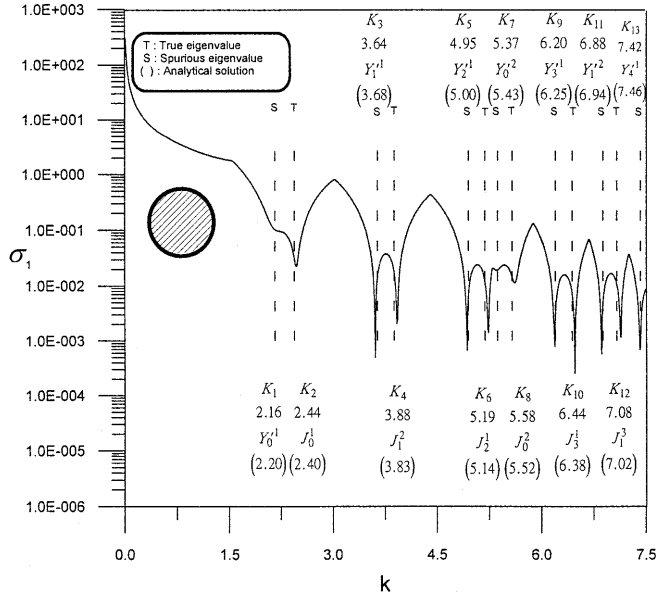

Fig. 10. The first minimum singular values σ_1 versus k using the $\begin{bmatrix} \bar{L}_r \\ U_r \end{bmatrix}$ matrices of dual BEM for the Dirichlet problem

conjunction with one additional equation from either $[\bar{L}_i]$ or $[U_r]$, the results are shown in Figs. 9 and 10. All the single spurious eigenvalues in Figs. 9 and 10 are filtered out as predicted analytically. The possible combination in choosing the base (dimension $2N \times 2N$) and one constraint (dimension $1 \times 2N$) for filtering out the single spurious eigenvalues is summarized in Table 4. Also, the performance grade is shown in this table according to numerical experiment. Figures 11, 12 and 13 show that the double spurious eigenvalues can be successfully filtered out by choosing the combination of $\begin{bmatrix} U_r \\ U_i^{(2)} \end{bmatrix}$, $\begin{bmatrix} \bar{L}_r \\ \bar{L}_i^{(2)} \end{bmatrix}$ and $\begin{bmatrix} \bar{L}_r \\ U_r^{(2)} \end{bmatrix}$, respectively. These results match well with analytical derivation. The possible combination in choosing the base and constraints for filtering out the double spurious eigenvalues is summarized in Table 5. Also, the performance grade is classified. To demonstrate the failure case in choosing the points with an intersection angle 180 degrees, Fig. 14 shows that the spurious eigenvalues of $Y_n(k), \quad n \geq 1$, cannot be filtered out as predicted analytically that $\sin(n\pi) = 0, n \geq 1$. For example, $Y_1^1(2.20)$ and $Y_2^1(3.38)$ spurious eigenvalues still exist.

Table 4. The possible combinations for filtering out the single spurious eigenvalues

Basic equations	Additional equation				
		$[U_i]_{1\times 2N}$ JJ	$[U_r]_{1\times 2N}$ YJ	$[L_i]_{1\times 2N}$ JJ′	$[L_r]_{1\times 2N}$ JY′
	$[U_i]_{2N\times 2N}$ JJ	Bad	Bad	Bad	Bad
	$[U_r]_{2N\times 2N}$ YJ	Excellent (Fig. 6)	Bad	Good (Fig. 7)	Fair (Fig. 8)
	$[L_i]_{2N\times 2N}$ JJ′	Bad	Bad	Bad	Bad
	$[L_r]_{2N\times 2N}$ JY′	Fair	Excellent (Fig. 10)	Excellent (Fig. 9)	Bad

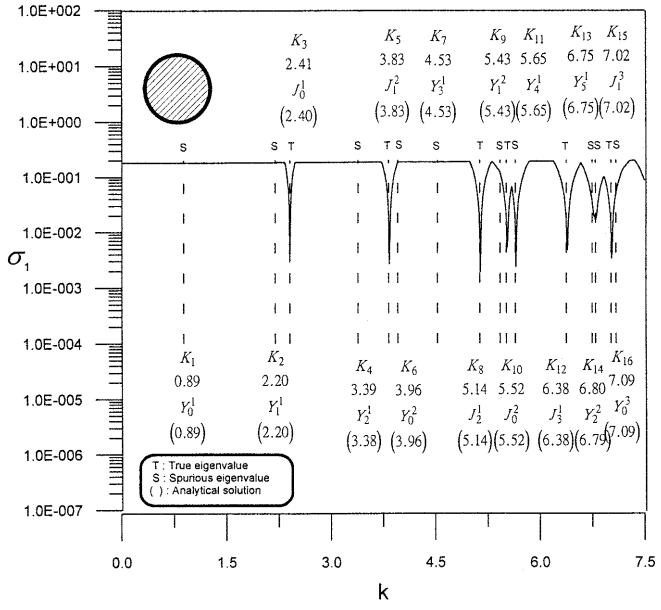

Fig. 11. The first minimum singular values σ_1 versus k using the $\begin{bmatrix} U_r \\ U_i \end{bmatrix}$ matrices of dual BEM for the Dirichlet problem

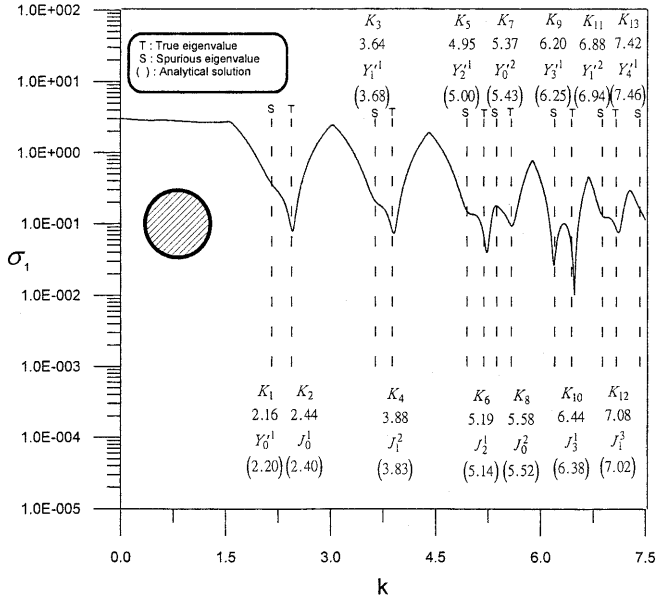

Fig. 12. The first minimum singular values σ_1 versus k using the $\begin{bmatrix} \bar{L}_r \\ \bar{L}_i \end{bmatrix}$ matrices of dual BEM for the Dirichlet problem

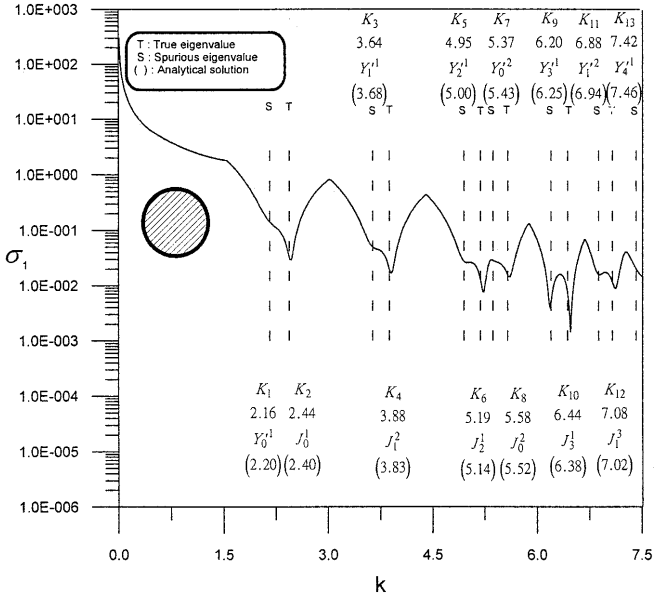

Fig. 13. The first minimum singular values σ_1 versus k using the $\begin{bmatrix} \bar{L}_r \\ U_r \end{bmatrix}$ matrices of dual BEM for the Dirichlet problem

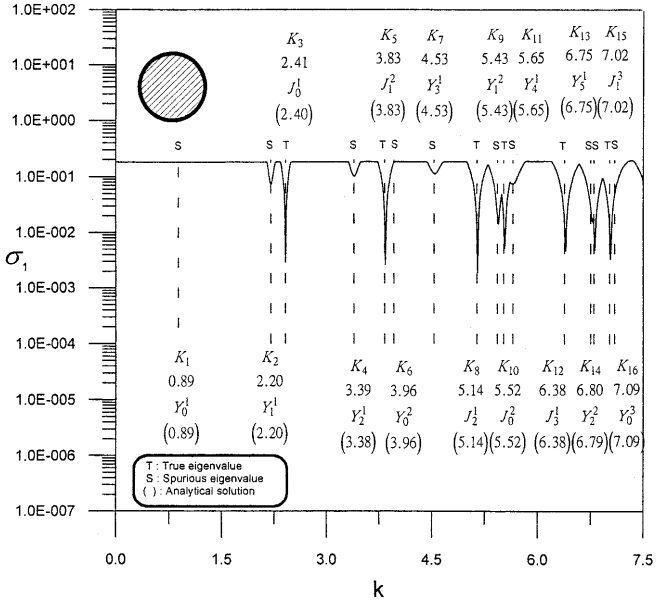

Fig. 14. The first minimum singular values σ_1 versus k using the $\begin{bmatrix} U_r \\ U_i \end{bmatrix}$ matrices of dual BEM for the Dirichlet problem with intersecting angle 180 degree

Table 5. The possible combinations of the more efficient method

	Additional equations				
Basic equations		$[U_i]_{2\times 2N}$ JJ	$[U_r]_{2\times 2N}$ YJ	$[L_i]_{2\times 2N}$ JJ′	$[L_r]_{2\times 2N}$ JY′
	$[U_i]_{2N\times 2N}$ JJ	bad	bad	bad	bad
	$[U_r]_{2N\times 2N}$ YJ	excellent (Fig. 11)	bad	good	fair
	$[L_i]_{2N\times 2N}$ JJ′	bad	bad	bad	bad
	$[L_r]_{2N\times 2N}$ JY′	fair	excellent (Fig. 13)	excellent (Fig. 12)	bad

6 Conclusions

An efficient method, termed mixed-part dual BEM, in conjunction with the SVD technique has been applied to determine the true and spurious eigenvalues of a circular cavity subjected to the Dirichlet boundary conditions. In comparing with the complex-valued BEM, not only half effort in constructing the matrix is required, but also a fewer size of dimension is needed. The failure cases in choosing the collocating points for circular cavity were designed analytically and demonstrated numerically. If the additional points were properly chosen, no more than two points were required. When one additional point was chosen, then we can succeed in filtering out single spurious roots. If the two points intersect an angle ϕ which makes $n\phi \neq \pi$, then we can filter out double spurious roots of the zeros $Y_n(k\rho)$ analytically. Numerical experiments were performed and matched well with analytical prediction. The true eigenvalues obtained by the efficient method agree very well with the exact solutions.

References

Chang JR, Yeih W, Chen JT (1999) Determination of the natural frequencies and natural modes of a rod using the dual BEM in conjunction with the superelement concept. Comput. Mech. 24: 29–40

Chen JT (1998) On ficitious frequencies using dual series representation. Mech. Res. Commun. 25: 529–534

Chen JT, Hong H-K (1999) Review of dual integral representations with emphasis on hypersingular integrals and divergent series. Trans. ASME Appl. Mech. Rev. 52: 17–33

Chen JT, Chen KH (1998) Dual integral formulation for determining the acoustic modes of a two-dimensional cavity with a degenerate boundary. Engng. Anal. Boundary Elements 21: 105–116

Chen JT, Wong FC (1997) Analytical derivations for one-dimensional eigenproblems using dual BEM and MRM. Engng. Anal. Boundary Elements 20: 25–33

Chen JT, Huang CX, Wong FC (2000a) Determination of spurious eigenvalues and multiplicities of true eigenvalues in the dual multiple reciprocity method using the singular value decomposition technique. J. Sound Vibration 230: 230–219

Chen JT, Kuo SR, Chen KH, Cheng YC (2000b) Comments on vibration analysis of arbitrary shaped membranes using nondimensional dynamic influence function. J. Sound Vibration 235(1): 156–170

Chen JT, Chen IL, Kuo SR, Liang MT (2000c) A new method for true and spurious eigensolutions of arbitrary cavities using the CHEEF method. J. Acoust. Soc. Am. Accepted

Chen JT, Chen KH, Chyuan SW (1999a) Numerical experiments for acoustic modes of a square cavity using dual BEM. Appl. Acoustics 57: 293–325

Chen JT, Huang CX, Chen KH (1999b) Determination of spurious eigenvalues and multiplicities of true eigenvalues using the real-part dual BEM. Comput. Mech. 24: 41–51

Chen JT, Kuo SR, Chen KH (1999c) A nonsingular integral formulation for the Helmholtz eigenproblems of a circular domain. J. Chinese Inst. Eng. 22: 729–739

De Mey G (1977) A simplified integral equation method for the calculation of the eigenvalues of Helmholtz equation. Int. J. Num. Meth. Engng. 11: 1340–1342

Goldberg JL (1991) Matrix Theory with Applications, McGraw-Hill, New York

Hutchinson JR (1991) Analysis of plates and shells by boundary collocation, in boundary elements analysis of plates and shells. In: Beskos DE (ed.), Springer-Verlag, Berlin, pp. 314–368

Hutchinson JR (1988) Vibration of plates, in boundary elements X. In: Brebbia CA (ed.), Springer-Verlag, Berlin, 4: 415–430

Hutchinson JR (1985) An alternative BEM formulation applied to membrane vibrations, in boundary elements VII. In: Brebbia CA, Maier G (eds.), Springer-Verlag, Berlin

Kamiya N, Andoh E, Nogae K (1996) A new complex-valued formulation and eigenvalue analysis of the Helmholtz equation by boundary element method. Adv. Engng. Software 26: 219–227

Kang SW, Lee JM, Kang YJ (1999) Vibration analysis of arbitrarily shaped membranes using non-dimensional dynamic influence function. J. Sound Vibration 221: 117–132

Katsikadelis JT, Nerantzaki MS (2000) A boundary-only solution to dynamic analysis of non-homogeneous elastic membrane. Comput. Modeling Engng. Sci. 1(3): 1–8

Kuo SR, Chen JT, Huang CX (2000a) Analytical study and numerical experiments for true and spurious eigensolutions of a circular cavity using the real-part dual BEM. Int. J. Numer. Meth. Engng. 48: 1401–1422

Kuo SR, Chung IL, Chen JT, Huang CX (2000b) Analytical study and numerical experiments for true and spurious eigensolutions of two-dimensional cavities using the dual multiple reciprocity method. Submitted

Kuo SR, Yeih W, Wu YC (2000c) Applications of generalized singular-value decomposition method on the eigenproblems using incomplete boundary element formulation. J. Sound Vibration 235(5): 813–845

Liou DY, Chen JT, Chen KH (1999) A new method for determining the acoustic modes of a two-dimensional sound field. J. Chinese Inst. Civil Hydraulic Engng. 11: 299–310 (in Chinese)

Schenck HA (1968) Improved integral formulation for acoustic radiation problems. J. Acoust. Soc. Am. 44: 41–58

Tai GG, Shaw RP (1974) Helmholtz equation eigenvalues and eigenmodes for arbitrary domains. J. Acoust. Soc. Am. 56: 796–804

Wu YC (1999) Applications of the generalized singular value decomposition method to the eigenproblem of the Helmholtz equation, Master Thesis National Taiwan Ocean University, Taiwan

Yeih W, Chang JR, Chang CM, Chen JT (1999a) Applications of dual MRM for determining the natural frequencies and natural modes of a rod using the singular value decomposition method. Adv. Engng. Software 30: 459–468

Yeih W, Chen JT, Chang CM (1999b) Applications of dual MRM for determining the natural frequencies and natural modes of an Euler–Bernoulli beam using the singular value decomposition method. Engng. Anal. Boundary Elements 23: 339–360

Yeih W, Chen JT, Chen KH, Wong FC (1997) A study on the multiple reciprocity method and complex-valued formulation for the Helmholtz equation. Adv. Engng. Software 29: 7–12